BMC Chemistry

RESEARCH

Open Access

Green synthesis of highly functionalized heterocyclic bearing pyrazole moiety for cancer-targeted chemo/radioisotope therapy

Kurls E. Anwer[1], Galal H. Sayed[1], Basma M. Essa[2*] and Adli A. Selim[3]

Abstract

New derivatives of heterocyclic bearing pyrazole moiety were synthesized (eight new compounds from 2 to 9) via green synthesis methods (microwave-assisted and grinding techniques). 4,6-Diamino-1,3-diphenyl-1*H*-pyrazolo[3,4-*b*]pyridine-5-carbonitrile (2) shows high anti-cancer activity against both HepG2 and HCT-116 with IC_{50} of 9.2 ± 2.8 and 7.7 ± 1.8 µM, respectively, which referenced to 5-Fu which is showing activity of 7.86 ± 0.5 and 5.35 ± 0.3 against both HepG2 and HCT-116, respectively. The cytotoxic activity against HCT-116 and HepG2 was slightly decreased and slightly increased, respectively, by a different pyrazole moiety (compound 5). Pharmacokinetics of compound 2 was carried out using the radioiodination technique in tumour-bearing Albino mice which shows good uptake at the tumour site. The biodistribution showed high accumulation in tumour tissues with a ratio of 13.7% ID/g organ after one hour in comparison with 2.97% ID/g organ at normal muscle at the same time point. As I-131 has maximum beta and gamma energies of 606.3 and 364.5 keV, respectively, therefore the newly synthesized compound 2 may be used for chemotherapy and TRT.

Keywords Microwave, Grinding, Pyrazole, Radioiodination, Dual cancer therapy

Introduction

Heterocyclic chemistry is a significant field of organic chemistry and has received a great deal of interest for its potential applications in industry, biology, and the advancement of human society [1–3]. Heterocyclic compounds typically have at least one heteroatom in their cyclic structures, such as nitrogen, sulfur, or oxygen can be made both naturally and artificially [3–5]. Molecules which provided by a heterocyclic nucleus mainly have improvements in salt formation properties and solubility which make an improvement in pharmacokinetic parameters [6, 7]. Additionally, it makes it easier to settle the pharmacophores and create several biologically active compounds such as anti-inflammatory, anti-tumor, antiviral and anti-bacterial compounds [8–13]. Compounds containing pyrazole moiety have received widely attention among heterocyclic compounds as a result of its extensive use in drug development research.

Pyrazole compounds are one of the most important heterocyclic derivatives widely used in petrochemical industry [14], catalytic and polymer manufacturing [15, 16]. Pyrazole derivatives have partially harmful effects on environment and humans and there are requirements for

*Correspondence:
Basma M. Essa
Basmamohamed24@yahoo.com
[1] Heterocyclic Synthesis Lab, Chemistry Department, Faculty of Science, Ain Shams University, Abbassia, Cairo 11566, Egypt
[2] Radioactive Isotopes and Generators Department, Egyptian Atomic Energy Authority, Cairo 13759, Egypt
[3] Labelled Compounds Department, Egyptian Atomic Energy Authority, Cairo 13759, Egypt

converting them into safe and useful products [17, 18]. During the last decades, derivatives of pyrazole showed wide-range of biological and pharmacological activities such as: anti-inflammatory, antagonist, analgesic, anthelmintic, anticancer, herbicidal, antiviral, antimitotic, antioxidant, insecticidal and antimicrobial activities [19–26]. Furthermore, synthetic heterocyclic compounds containing nitrogen atoms have proven to have significant and diverse therapeutic potential for cancer which is one of the major causes of death worldwide [27].

Green chemistry is the chemical processes design science that eliminate or reduce the hazardous compounds generation. It prevents the pollution at a molecular level. Microwave and grinding techniques use in heterocyclic compounds synthesis are also important branch from green chemistry techniques. One-pot multicomponent reactions [28, 29] are one of the most important tools for synthesis with facile execution, the effectiveness for its productivity and highly diverse products generation in a single running and from easily starting materials. So, such techniques have much more attention because of its safe on the environment, improvement of the reactions yield and time, more convenient, and easily synthetic procedures which are highly energy efficient. Comparing both microwave irradiation and grinding techniques with the conventional heating method; it's clear that microwave irradiation and grinding techniques are more environmentally tolerant, easily controlled and friendly environmental. As advantage, many heterocyclic reactions were carried out in shorter reaction time, higher yield, and milder and cleaner conditions [30–32]. So now, this green synthesis type is considered as significant technique in heterocyclic chemistry synthesis because of its economy, simplicity and mild conditions. as aforementioned about heterocycles derivatives, and according to their favorite applications in biology and industry; more efforts in synthesizing novel heterocycles derivatives still continued [33–40].

Nuclear medicine technology is essential for developing both the search for disease treatments and the development of novel drugs. Iodine-131 is one of the most used radioisotopes in nuclear medicine. I-131 decays to the extremely stable xenon-131 with a half-life of 8.03 days. A negative beta particle as well as gamma photons are released during the decay process. The major beta emission has average and maximum energies of 191.5 keV and 606.3 keV, respectively, while the primary photon (gamma emission) has an energy of 364.5 keV [41], therefore it used in targeted radionuclide therapies (TRTs) [42].

In this study, designing and synthesizing enamino pyrazole derivative was reported as starting material via one-pot multicomponent reaction using microwave and grinding techniques. On the other hand, the reactions were pressed using thermal method according to literature method [43, 44]. Comparison between the percentage yields and consumed times, which resulting from the two techniques were performed. The yield economy "YE", atom economy "AE", reaction mass efficiency "RME" and optimum efficiency "OE" were used for comparison between the consumed times and the percent of the yields resulting from these techniques. The various synthesized compounds were illustrated by using different spectroscopic and analytical tools. The newly compounds were screened *in-vitro* anticancer against two cancer cell lines, namely, hepatocellular carcinoma (HepG2), and colorectal carcinoma (HCT-116). Radioiodination technique was used to study the pharmacokinetic of the most effective synthesized compound and also to be used as a potential agent as TRT for cancer tissues (Scheme 1).

Experimental

Synthesis

All solvents, reagents and chemicals were bought from Sigma Aldrich. TLC (Merck Kiesel gel 60F254, BDH) to monitor the progress of all synthesized compounds. Microwave reactions were carried out with microwave reactor Anton Paar (monowave 300). All melting points were measured on a digital Stuart electric melting point apparatus "SMP3". Infrared spectra measurements were determined using KBr disks on PerkinElmer 293 spectrophotometer. The ^{1}H-NMR and ^{13}C-NMR spectra were measured on a Varian Mercury 75 MHz spectrometer. A GC-2010 Shimadzu Gas chromatography mass spectrometer (EI, 70 eV) was used for Mass spectrometry measurements. A Perkin-Elmer CHN-2400 analyzer was used for elemental microanalyses (CHN). No-carrier-added [^{131}I] NaI was received as a gift from RPF (Radioisotopes-Production-Facility), Egyptian Atomic Energy Authority (EAEA). A NaI (Tl) scintillation counter (Scaler Ratemeter SR7 model, the United Kingdom) was used for γ-ray radioactivity measurement.

General procedure for preparation of compounds (2–4)

A mixture of enaminonitrile 1 (10 mmol., 2.6 g) and each of malononitrile (10 mmol., 0.66 g), cyanoacetamide (10 mmol., 0.84 g) and/or chloroacetic acid (10 mmol., 0.94 mL) in presence of sodium ethoxide (0.4 g sodium ethoxide in 2 mL ethanol) was irradiated for 2–2.5 min. The reaction mixture after cooling was poured into ice water, formed solid was filtrated, and then recrystallized from the proper solvent to give compounds 2–4, respectively.

4,6-Diamino-1,3-diphenyl-1H-pyrazolo[3,4-b]pyridine-5-carbonitrile (2) Black crystals from ethanol.

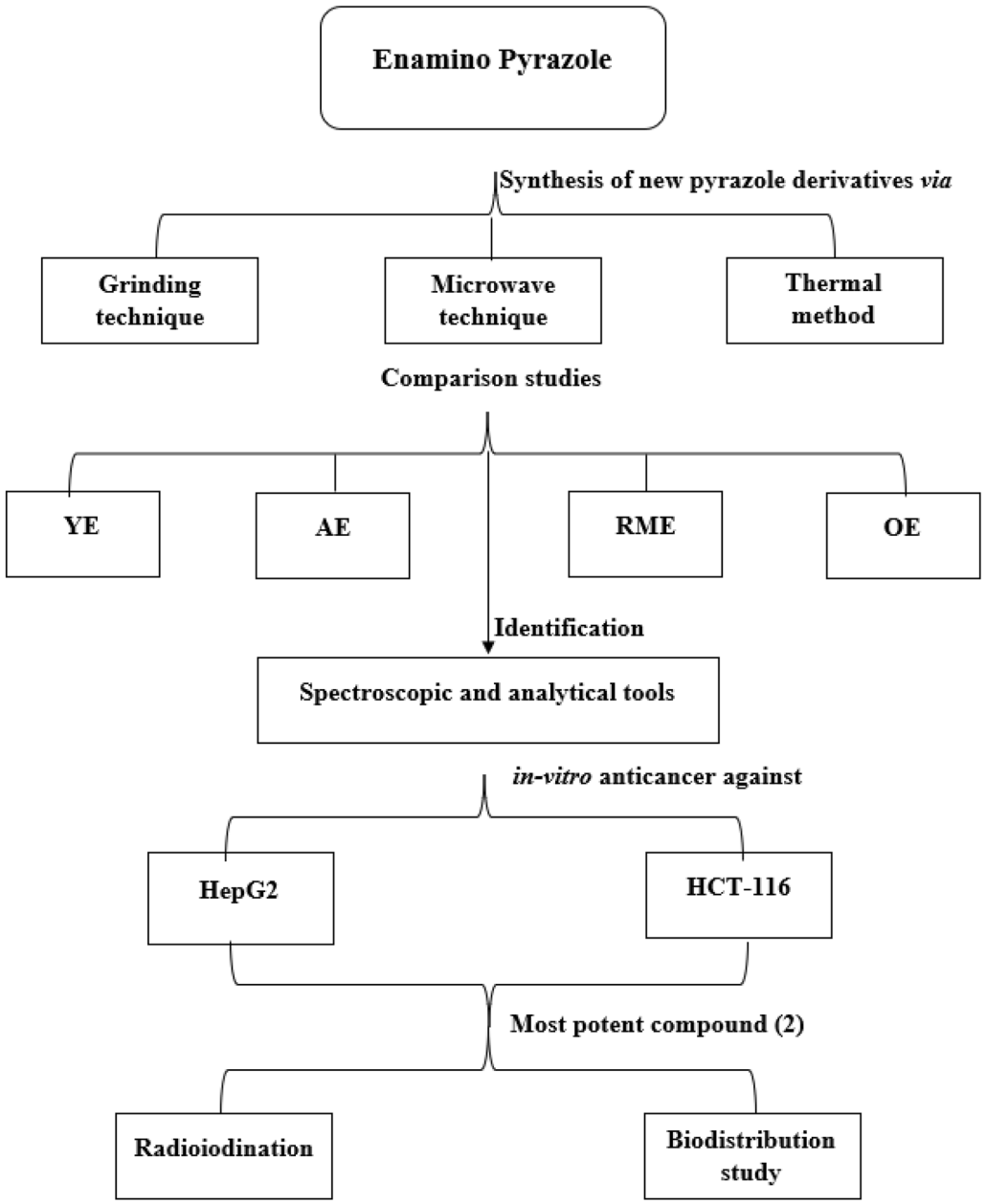

Scheme 1 Working plan

Yield 96.7%. IR (cm^{-1}) υ: 3442, 3315, 3290 ($2NH_2$), 2169 (CN), 1633, 1601 (C=C). ^{1}H-NMR (300 MHz, DMSO-d_6) δ (ppm): 6.72–7.87 (m, 10H; Ar–H), 10.32 (s, 4H, $2NH_2$; D_2O exchangeable). MS (m/z): 326 (M^+, 40.9%). Anal. Calcd. for $C_{19}H_{14}N_6$: C, 69.92; H, 4.32; N, 25.75; Found: C, 69.88; H, 4.14; N, 25.98%.

4,6-Diamino-1,3-diphenyl-1H-pyrazolo[3,4-b]pyridine-5-carboxamide (3) Orange crystals from ethanol. Yield 94.5%. IR (cm^{-1}) υ: 3445, 3309, 3281 (NH_2), 1658 (C=O), 1595, 1564 (C=N). ^{1}H-NMR (300 MHz, DMSO-d_6) δ (ppm): 6.72–7.86 (m, 10H; Ar–H), 8.89 (s, 4H, $2NH_2$; D_2O exchangeable), 11.24 (s, 2H, $CONH_2$; D_2O-exchangeable); ^{13}C-NMR (75 MHz, DMSO-d_6) δ (ppm): 117.1, 123.9, 130.7, 133.0, 133.7, 134.2, 140.9, 141.6, 150.4 and 162.3. MS (m/z): 344 (M^+, 13.3%). Anal. Calcd. for $C_{19}H_{16}N_6O$: C, 66.27; H, 4.68; N, 24.40; Found: C, 66.05; H, 4.74; N, 24.51%.

4-Amino-1,3-diphenyl-1,6-dihydropyrrolo[2,3-c]pyrazole-5-carboxylic acid (4) Red crystals from ethanol. Yield 95.5%. IR (cm^{-1}) υ: 3476 (OH), 3414, 3311 (NH_2), 3223 (NH), 1709 (C=O), 1645(C=N), 1593(C=C). ^{1}H-NMR (300 MHz, DMSO-d_6) δ (ppm): 5.08 (s, 2H, NH_2; D_2O exchangeable), 6.72–7.89 (m, 10H; Ar–H), 10.0 (s, 1H, NH; D_2O exchangeable), 10.40 (s, 1H, OH; D_2O exchange). MS (m/z): 318 (M^+, 9.8%). Anal. Calcd. for $C_{18}H_{14}N_4O_2$: C, 67.92; H, 4.43; N, 17.60; Found: C, 67.81; H, 4.44; N, 17.51%.

4,6-Diphenyl-1,6-dihydropyrazolo[3,4-c]pyrazol-3-amine (5)

A mixture of enaminonitrile 1 (10 mmol., 2.6 g) and hydrazine hydrate (10 mmol., 0.5 mL) was irradiated for 4 min. The reaction mixture after cooling was poured into ice water, formed solid was filtrated, and recrystallized from methanol to give compound 5.

Brown crystals. Yield 94.1%. IR (cm^{-1}) υ: 3385, 3313 (NH_2), 3201 (NH), 1627, 1592 (C=N). ^{1}H-NMR (300 MHz, DMSO-d_6) δ (ppm): 6.73–7.87 (m, 10H; Ar–H), 8.68 (s, 1H, NH; D_2O exchangeable), 10.31 (s, 2H, NH_2; D_2O exchangeable). MS (m/z): 275 (M^+(8.1%). Anal. Calcd. for $C_{16}H_{13}N_5$: C, 69.80; H, 4.76; N, 25.44; Found: C, 69.67; H, 4.88; N, 25.45%.

4-Amino-1,3-diphenyl-1,7-dihydro-6H-pyrazolo[3,4-d] pyrimidin-6-one (6)

A mixture of enaminonitrile 1 (10 mmol., 2.6 g), urea (10 mmol., 0.66 g) and acetic acid (2 mL) was irradiated for 3 min. The reaction mixture after cooling was poured into ice water, formed solid was filtrated, and recrystallized from toluene to afford compound **6**.

Red crystals. Yield 93.3%. IR (cm^{-1}) υ: 3456, 3312 (NH_2, NH), 1688 (C=O), 1611 (C=N). ^{1}H-NMR (300 MHz, DMSO-d_6) δ (ppm): 6.69–7.92 (m, 10H; Ar–H), 9.55 (s, 2H, NH_2; D_2O exchangeable), 10.28 (s, 1H, NH; D_2O exchangeable); ^{13}C-NMR (75 MHz, DMSO-d_6) δ (ppm): 117.1, 123.3, 130.2, 133.6, 134.1, 134.2, 140.9, 141.6, 150.4 and 159.8. MS (m/z): 303 (M^+, 37.7%). Anal. Calcd. for $C_{17}H_{13}N_5O$: C, 67.32; H, 4.32; N, 23.09; Found: C, 67.14; H, 4.39; N, 23.44%.

General procedure for preparation of compounds (7 & 8)

A mixture of enaminonitrile 1 (10 mmol., 2.6), and each of thiourea (10 mmol., 0.76 g) and/ or benzaldehyde (10 mmol., 1.06 mL) in the presence of sodium ethoxide (0.4 g sodium ethoxide in 2 mL ethanol) was irradiated for 2.5 min. The reaction mixture after cooling was poured into ice water, formed solid was filtrated, and then recrystallized from the proper solvent to give compounds 7&8.

4-Amino-1,3-diphenyl-1,7-dihydro-6H-pyrazolo[3,4-d] pyrimidine-6-thione (7) Red crystals from toluene. Yield 96.6%. IR (cm^{-1}) υ: 3397, 3311 (NH_2), 3200 (NH), 1600, 1593 (C=N), 1287 (C=S). ^{1}H-NMR (300 MHz, DMSO-d_6) δ (ppm): 6.72–7.87 (m, 10H, Ar–H), 10.33 (s, 2H, NH_2, D_2O exchangeable), 13.14 (s, 1H, NH, D_2O exchangeable). ^{13}C-NMR (75 MHz, DMSO-d_6) δ (ppm): 117.2, 123.9, 130.7, 133.0, 133.8, 134.1, 134.2, 140.9, 141.6, 150.5 and 189.1. MS (m/z): 319 (M^+, 10.7%). Anal. Calcd. for $C_{17}H_{13}N_5S$: C, 63.93; H, 4.10; N, 21.93; S, 10.04; Found: C, 63.74; H, 4.22; N, 22.04; S, 10.00%.

4-Ethoxy-1,3,6-triphenyl-1H-pyrazolo[3,4-d]pyrimidine (8)

Brown crystals from ethanol. Yield 95.2%. IR (cm^{-1}) υ: 1633, 1600 (C=N). ^{1}H-NMR (300 MHz, DMSO-d_6) δ (ppm): 1.31 (t, J=6.0 Hz, 3H; $\underline{CH_3}CH_2$), 4.20 (q, J=6.6 Hz, 2H; $CH_3\underline{CH_2}$), 6.72–7.86 (m, 15H; Ar–H); ^{13}C-NMR (75 MHz, DMSO-d_6) δ (ppm): 15.9, 56.8, 111.9, 118.8, 125.6, 127.9, 127.9, 135.7, 136.6 and 145.2. MS (m/z): 392 (M^+, 14.1%). Anal. Calcd. for $C_{25}H_{20}N_4O$: C, 76.51; H, 5.14; N, 14.28; Found: C, 76.43; H, 5.28; N, 14.01%.

6-(5-Amino-1,3-diphenyl-1H-pyrazol-4-yl)-1,3-diphenyl-1H-pyrazolo[3,4-d]pyrimidin-4-amine (9)

A mixture of enaminonitrile 1 (10 mmol., 2.6 g) and TEA (2 mL) was irradiated for 3 min. The reaction mixture after cooling was poured into ice water, formed solid was filtrated, and recrystallized from methanol to afford compound 9.

Red crystals. Yield 97.4%. IR (cm^{-1}) υ: 3427, 3311 (NH_2), 1591 (C=N). ^{1}H-NMR (300 MHz, DMSO-d_6) δ (ppm): 6.72–7.86 (m, 20H; Ar–H), 9.41 (s, 2H, NH_2; D_2O exchangeable), 10.57 (s, 2H, NH_2; D_2O exchangeable); ^{13}C-NMR (75 MHz, DMSO-d_6) δ (ppm): 112.0, 118.7, 125.6, 127.9, 128.6, 129.1, 135.9, 136.4 and 145.3. MS (m/z): 520 (M^+, 24.7%). Anal. Calcd. for $C_{32}H_{24}N_8$: C, 73.83; H, 4.65; N, 21.52; Found: C, 73.77; H, 4.72; N, 21.51%.

Comparison between conventional, grinding and microwave methods

The conventional, grinding and microwave reaction times were showed in Table 1. The yield economy (YE) was used as a term to determine the conventional, grinding, and microwave synthetic different efficiencies of the same reaction. Calculation of YE was occurred through: $E = \frac{yield\%}{Reaction\ time"min"}$. YE was used to provide the yields obtained conclusively enhanced under the conventional,

Table 1 Show the comparison in terms of physical data between the synthesized compounds under grinding and microwave techniques

		2	3	4	5	6	7	8	9
Melting point (°C)	Found	100–102	122–124	172–174	140–142	104–106	222–224	138–140	160–162
	Lit*	100–102	120–122	170–172	140–142	106–108	220–222	138–140	160–162
Time "min"	Con	240	240	180	180	180	180	240	420
	G	10	12	14	17	16	13	11	14
	M.W	2	2.5	2	4	3	2.5	3.5	3
Yield %	Con	80	75	78	76	76	75	81	85
	G	89.4	89.1	88.9	87.3	88.7	86.0	89.5	90.8
	M.W	96.7	94.5	95.5	94.1	93.3	96.6	95.2	97.4
YE	Con	0.3333	0.3125	0.4333	0.4222	0.4222	0.4167	0.3375	0.2024
	G	8.94	7.43	6.35	5.14	5.54	6.62	7.50	6.49
	M.W	48.35	37.80	47.75	23.53	31.10	38.64	27.20	32.47
RME	Con	66.19	62.62	58.78	67.66	60.60	58.93	73.16	66.27
	G	73.97	74.39	66.99	77.73	70.72	67.57	80.83	76.03
	M.W	80.01	78.90	71.96	83.78	74.39	75.90	85.99	81.56
OE	Con	0.6619	0.6262	0.6562	0.7627	0.6400	0.6207	0.7634	0.6884
	G	0.7400	0.7439	0.7478	0.8762	0.7469	0.7117	0.8434	0.7898
	M.W	0.8001	0.7890	0.8033	0.9444	0.7856	0.7995	0.8972	0.8473
AE		100	100	89.58	88.71	94.69	94.94	95.84	96.26

**Lit*. literature value, YE yield economy, RME reaction mass efficiency, OE optimum efficiency, AE atom economy, *Con*. conventional, *G*. grinding, *M.W*. microwave

grinding and microwave conditions.RME $= \frac{Wt\ of\ isolated\ product}{Wt\ of\ reactants}$. OE was used for the direct comparisons between the two reaction types and can be calculated through$OE = \frac{RME}{AE} x100$. So, the yield economy (YE) can be considered as a metric to enhancing the conversion efficiencies of these two different synthetic methods of the same reaction. The reaction theoretical maximum efficiency was represented by using AE, while, RME gives the observed mass efficiency. The grinding and microwave reactions atom economy (AE) have the same values due to using two different reaction conditions to obtain the same desired compounds, as shown in Table 1.

In vitro *anticancer evaluation*

Cell line

Hepatocellular carcinoma (HepG2), and colorectal carcinoma (HCT-116). The cell lines were obtained from ATCC via Holding company for biological products and vaccines (VACSERA), Cairo, Egypt.

Chemical reagents

The reagents RPMI-1640 medium, MTT and DMSO (sigma co., St. Louis, USA), Fetal Bovine serum (GIBCO, UK). 5-Fluorouracil was used as a standard anticancer drug for comparison.

MTT assay (1)

HepG2 and (HCT-116 were used to determine the inhibitory effects of compounds on cell growth using the MTT assay. The relative cell viability in percentage was calculated as (A570 of treated samples/A570 of untreated sample) X 100.

Preparation of [^{131}I]iodo-pyrazole derivative

Radioiodination of compound **2** was performed using different values of the synthesized pyrazole derivative (25–400 µg) solutions, then 200 µL of chloramine-T (CAT) solution -freshly prepared- containing (100–600 µg). Then, 10 µL of (4 MBq) [^{131}I]NaI was dropped to the reaction mixture, after that pH values were studied in a range from 4 to 9. The mixture was kept at ambient temperature for 24 h.

Assessment of radiochemical purity

Formation of [^{131}I]iodo-pyrazole derivative was assessed using TLC in a mobile phase chloroform: methanol (3: 1). 5 µL from reaction was added at the spotted point at the lower edge of the paper strip, then in ascending manner TLC was developed prepared using chloroform: methanol (3: 1 v/v). [^{131}I] iodo-pyrazole derivative was migrate to R_f = 0.9; while free iodide remained at the spotted area. Then RCP was calculated.

In-vivo evaluation of [^{131}I]iodo-pyrazole derivative

Biodistribution studies was performed under the Animal Ethics Committee criteria, EAEA [45–47]. Swiss Albino mice aged three months weight 20–25 g were taken as a gift from the animal house of Egyptian Atomic Energy Authority. Ehrlich-Ascites-Carcinoma cell line (EAC) was taken from a female mouse mammary carcinoma, then used for induction of the tumour [34, 48]. 50 µL from diluted EAC cell line was injected intramuscularly in the right Albino swiss mouse thigh 5 days. Six groups of three mice each were injected intravenously at the mice tail. The substrate concentration (compound 2) in the intravenous injection was 6.14×10^{-4} mM, while the injected activity in each mice equal 0.4 MBq ([^{131}I]NaI). Then the mice were anaesthetized with isoflurane, weighted and sacrificed using cervical dislocation method at different time intervals (0.25, 0.5, 1, 2, 3, and 24 h) and the organs were dissected, weighed and counted. Then results were calculated as % ID/g.

Results and discussion

Synthesis

Microwave and grinding techniques were used for heterocyclic synthesis to obtain an environmentally friendly methods are in accordance with the green chemistry principles [49–51]. Our objective was to develop a synthetic method for the reaction of 5-amino-1,3-diphenyl-1H-pyrazole-4-carbonitrile (1) with different nucleophilic and electrophilic reagents using microwave and grinding techniques. The reactions were repeated using conventional technique with the similar outcome. The bifunctional starting material 1 can be used as a key intermediate in interesting bicyclic compounds synthesis, via its irradiation with different nucleophilic reagents namely malononitrile, cyanoacetamide and/or chloroacetic acid in presence of sodium ethoxide producing pyrazolopyridine and pyrazolopyrrole derivatives 2–4, respectively. Formation of di-enaminonitrile derivative 2 occurred through the condensation reaction between the amino group and malononitrile to form the intermediate (A), which undergo ring closure formed the expected compound. The structure of compound 2 was confirmed from its IR spectrum, which displayed bands at 3442, 3315, 3290 cm^{-1} characteristics for the NH_2 group. Its ^{1}H-NMR spectrum showed a peak corresponding to $2NH_2$ at 10.32 ppm. Its mass spectrum revealed a molecular ion peak at 326 (M^+) corresponding to $C_{19}H_{14}N_6$. However, formation of compound 3 may takes place through the nucleophilic attack of the amino group on the cyano group of cyanoacetamide to form the intermediate (B), which underwent ring closure to produce the expected derivative. While the structure of compound 3 was supported from its IR spectrum, which was devoid of CN band and displayed band at 1658 cm^{-1} characteristics for the C=O group. Its ^{1}H-NMR spectrum display peaks corresponding to $2NH_2$ and $CONH_2$ at 8.89 and 11.24 ppm, respectively. Its ^{13}C-NMR spectrum showed a peak corresponding to C=O at 162.3 ppm. Its mass spectrum revealed a molecular ion peak at 344 (M^+) corresponding to $C_{19}H_{16}N_6O$. Also, in case of compound 4 formation, chloroacetic acid reacted with the amino group forming the intermediate (C) through the elimination of one HCl molecule and then ring closure takes place. Also, IR spectrum of compound 4 showed disappearance of CN band in its IR spectrum and displayed bands at 3223 and 1709 cm^{-1} characteristics for the NH and C=O groups, respectively. Its ^{1}H-NMR spectrum display peaks at 5.08, 10.00 and 10.40 ppm corresponding to NH_2, NH and OH, respectively. Its mass spectrum revealed a molecular ion peak at 318 (M^+) corresponding to $C_{18}H_{14}N_4O_2$. Furthermore, compound 1 was subjected to the reaction with hydrazine hydrate in microwave to produce pyrazolopyrazole derivative 5 (Scheme 2). Furthermore, the structure of compound 5 was illustrated from its IR spectrum, which was devoid of CN band and revealed bands at 3385, 3313 and 3201 specifics for NH_2 and NH groups, respectively. Its ^{1}H-NMR spectrum display peaks at 8.68 and 10.31 ppm corresponding to NH and NH_2, respectively. Its mass spectrum revealed a molecular ion peak at 275 (M^+) corresponding to $C_{16}H_{13}N_5$.

While, pyrazolopyrimidin-6-one 6 was obtained through the condensation reaction between the amino group and urea to form the intermediate (D) through the elimination of one molecule of ammonia which undergo ring closure formed the expected compound. However, the structure of compound 6 was illustrated from its IR spectrum, which was devoid of CN band and revealed band at 1688 specifics for C=O group. Its ^{1}H-NMR spectrum display peaks at 9.55 and 10.28 ppm corresponding to NH_2 and NH, respectively. Its ^{13}C-NMR spectrum showed a peak corresponding to C=O at 159.8 ppm. Its mass spectrum revealed a molecular ion peak at 303 (M^+) corresponding to $C_{17}H_{13}N_5O$. Pyrazolopyrimidin-6-thione 7 was furnished in the same manner through the intermediate (E). While the structure of compound 7 was supported from its IR spectrum, which was devoid of CN band and displayed band at 3200 and 1287 corresponding to NH and C=S groups, respectively. Its ^{1}H-NMR spectrum display peaks at 10.33 and 13.14 ppm corresponding to NH_2 and NH, respectively. Its ^{13}C-NMR spectrum showed a peak corresponding to C=S at 189.1 ppm. Its mass spectrum revealed a molecular ion peak at 319 (M^+) corresponding to $C_{17}H_{13}N_5S$. Noteworthy, pyrazolopyrimidine derivative 8 was formed through the compound 1 irradiation with benzaldehyde in the

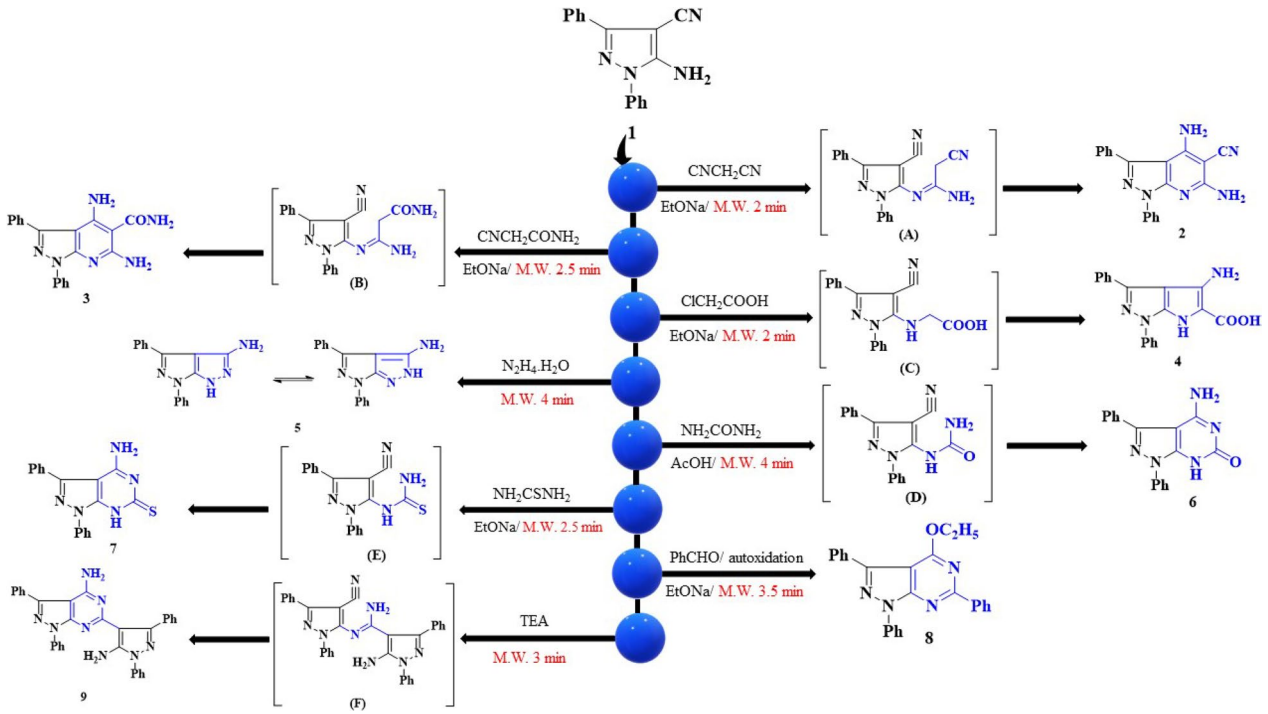

Scheme 2 Synthesis of pyrazolopyridine (2, 3), pyrazolopyrrole (4), pyrazolopyrazole (5), and pyrazolopyrimidine (6–9) derivatives

presence of sodium ethoxide. Furthermore, the structure of compound 8 was illustrated from its ^{1}H-NMR spectrum display peaks at 1.31 and 4.20 corresponding to CH_3 and CH_2 groups, respectively. Its ^{13}C-NMR spectrum showed a peak corresponding to CH_3 and CH_2 at 15.9 and 56.8 ppm, respectively. Its mass spectrum revealed a molecular ion peak at 392 (M^+) corresponding to $C_{25}H_{20}N_4O$. However, compound 9 formation takes place through the two molecules of compound 1 condensation, where the first molecule amino group attacks the second molecule cyano group, producing the intermediate (F) followed by ring closure (Scheme 2). However, the structure of compound 9 was illustrated from its ^{1}H-NMR spectrum display peaks at 9.41 and 10.57 ppm corresponding to $2NH_2$ groups. Its mass spectrum revealed a molecular ion peak at 520 (M^+) corresponding to $C_{32}H_{24}N_8$.

Table 2 Anticancer activity of the synthesized pyrazole derivatives against HepG2 and HCT-116 cell lines

Comp	*In-vitro* Cytotoxicity IC_{50} (μM)[a]	
	HepG2	HCT-116
5-Fu[b]	7.86 ± 0.5	5.35 ± 0.3
2	9.2 ± 2.8	7.7 ± 1.8
3	22.8 ± 2.1	29.4 ± 2.3
4	14.5 ± 2.8	15.2 ± 2.4
5	8.8 ± 5.1	13.8 ± 3.9
6	91.4 ± 4.2	51.0 ± 2.7
7	10.2 ± 2.1	13.1 ± 2.3
8	12.1 ± 5.1	17.4 ± 3.9
9	55.7 ± 2.7	33.6 ± 2.1

[a] IC_{50} (μM): 1–10 (very strong). 11–20 (strong). 21–50 (moderate). 51–100 (weak) and above 100 (non-cytotoxic)

[b] 5-Fu: 5-Fluorouracil

In-vitro anticancer evaluation

The synthesized pyrazole derivatives were *in-vitro* examined for its cytotoxicity against two types of human cancer cells (HepG2 and HCT-116) as shown in Table 2. their cytotoxic ability was compared with 5-Fu as a reference. Results showed that the tested compound 2 has the highest cytotoxic effect against the two assessed cell lines showing an obvious cytotoxic activity. The obtained IC_{50} values of compound 2 were 9.2 ± 2.8 and 7.7 ± 1.8 μM against HepG2 and HCT-116, respectively.

Structure–Activity Relationship (SAR)

In this study, a series of heterocyclic bearing Pyrazole moiety derivatives were synthesized and their cytotoxicity were evaluated against two cancer cell lines (HepG2 and HCT-116). Various derivatives were synthesized

from 5-amino-1,3-diphenyl-1H-pyrazole-4-carbonitrile (compound 1). The tested compounds results showed that exhibited very strong, strong, moderate, or weak anticancer activities against the tested cell lines. First, malononitrile was added forming pyridine moiety having diamino and cyano group (compound 2) appeared to have the highest biological activity against both cell lines. Further modifications were implemented which resulted in drastic decrease in activity. The activity of compounds 2 may be related to the core of compound which is pyrazolopyridine ring in addition to the cyano group presence at position 5 of the pyridine ring which is an electron-withdrawing group, in addition to the two amino groups presence at positions 4 and 6 of compound 2. However, the addition of hydrazine hydrate having another pyrazole moiety (compound 5) caused slight decrease in the cytotoxic activity against HCT-116 and slight increase against HepG. While the activity of compounds 5 may be related to the pyrazolopyrazole ring in addition to the two amino groups presence at positions 3 and the NH of the ring of compound 5. However, the activity of compounds 7 may be related to pyrazolopyrimidine ring in addition to the C=S group presence at position 7 of the pyrimidine ring, which is a rich by electron centres, in addition to the two amino groups presence at position 4 of compound 7. Further modifications using cyanoacetamide, chloroacetic acid, thiourea, benzaldehyde, and TEA caused some decrease in the cytotoxic activity. (Additional file 1).

Radioiodination of pyrazole derivative

Compound 2 can be used as a chemotherapeutic agent because it is the highest cytotoxic synthesized compound against both HepG2 and HCT-116 cell lines. Compound 2 was radiolabeled with iodine-131 to evaluate its biodistribution in animal models and also to be studied to carry the therapeutic radioisotope (iodine-131) to the target site (cancer tissues) for targeted radio therapy (TRT). The highest radiochemical purity of radioiodinated compound 2 was obtained by optimization of all parameters affecting the radioiodination process. The electrophilic substitution of iodine-131 was carried out in the presence of an oxidizing agent (chloramine-T). Chloramine-T, which converts iodide ion to iodonium ion [52], has a clear impact on the process of radioiodination, also an electrophilic substitution was happen by the permission from the oxidizing agent. 400 µg from CAT was the optimum amount required to create the highest RCP of 91.74% (Fig. 1). Different CAT amounts may cause undesirable oxidative byproduct and Insufficient oxidation of I-131 by increasing or decreasing of its value, respectively [53]. pH value is a main factor which affect the RCP. The RCP was decreased in acidic media and increased around

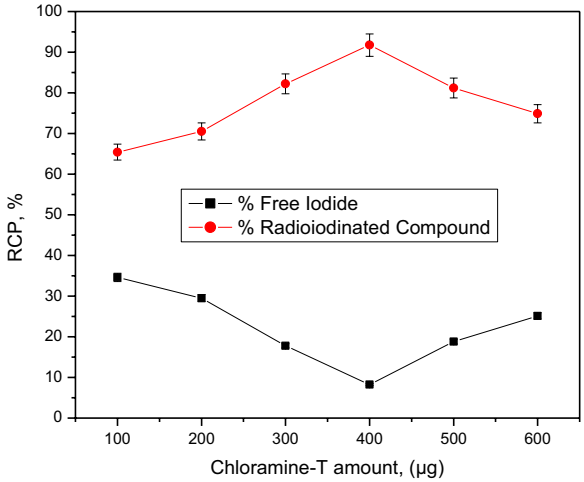

Fig. 1 Effect of CAT amount on RCP of [^{131}I]I-compound 2. Reaction conditions: 100 µg compound 2, pH 6, 10 µL (3.7 MBq) [^{131}I] NaI solution for 30 min at ambient temperature, $n=3$ independent experiments

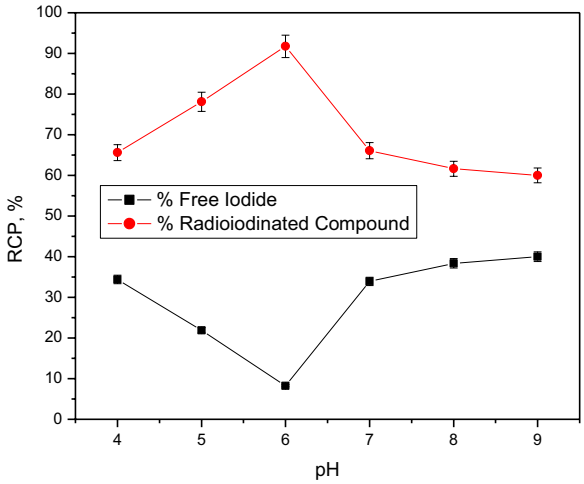

Fig. 2 Effect of pH amount on RCP of [^{131}I]I-compound 2. Reaction conditions: 400 µg CAT, 100 µg compound 2, 10 µL (3.7 MBq) [^{131}I] NaI solution for 30 min at ambient temperature, $n=3$ independent experiments

neutral values then decreases again towards basic media (Fig. 2). The formation of hypoiodite (IO^-) ion and iodate (IO_3^-) ions may be the cause of this decrease in RCP value [54]. Figure 3 illustrate the effect of compound 2 amount on the RCP. The maximum RCP was obtained at 100 µg from compound 2, this amount can react with all ions of iodonium in the reaction. By increasing the amount of substrate, the RCP still stable around the highest yield. Figure 4 showed the time effect on the radioiodination process which indicates its fastness. The reaction stability study was done for 24 h.

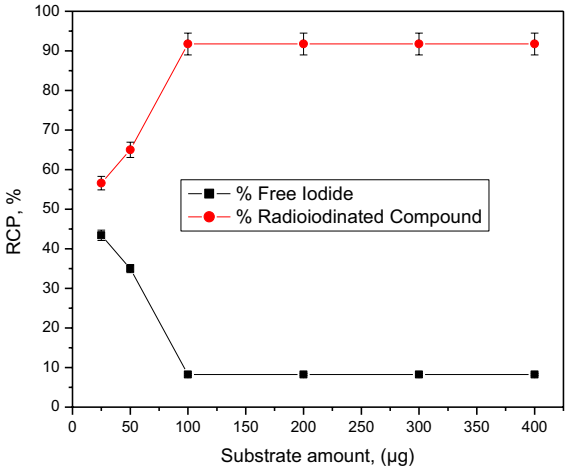

Fig. 3 Effect of compound 2 amount on RCP of [^{131}I]I-compound 2. Reaction conditions: 400 µg CAT, pH 6, 10 µL (3.7 MBq) [^{131}I]NaI solution for 30 min at ambient temperature, $n=3$ independent experiments

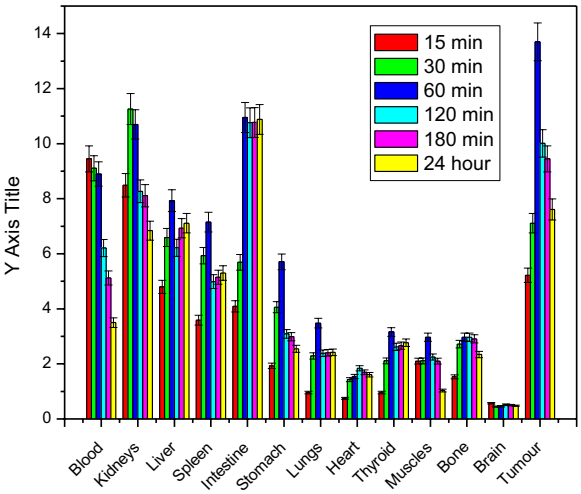

Fig. 5 Biological distribution of [^{131}I] I- compound 2 in solid tumor-bearing mice. $n=3$ independent experiments

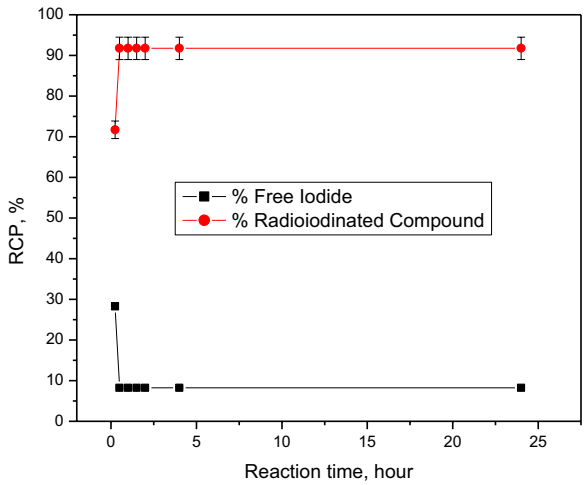

Fig. 4 Effect of reaction time on RCP of [^{131}I] I-compound 2. Reaction conditions: 400 µg CAT, 100 µg compound 2, pH 6, 10 µL (3.7 MBq) [^{131}I] NaI solution at ambient temperature, $n=3$ independent experiments

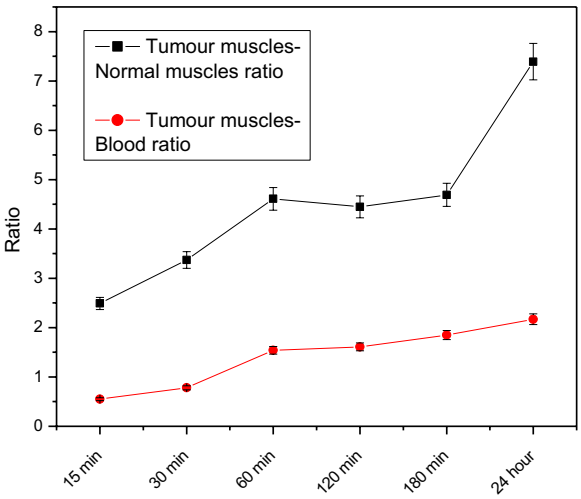

Fig. 6 T/NT of [^{131}I] I- compound 2 in solid tumour-bearing mice (Tumour muscles/Normal muscles, and Tumour muscles/Blood). $n=3$ independent experiments

Biodistribution study of [^{131}I]iodo-pyrazole derivative

The biodistribution data of [^{131}I]I- compound **2** (Fig. 5) in tumour-bearing mice at different times (0.25, 0.5, 1, 2, 3, and 24 h) post-injection reveals that excretion of [^{131}I] I-compound 2 occurs via both urinary and hepatobiliary pathways due to relatively high uptake for kidney and liver over the time. As shown in Fig. 5 [^{131}I]I-compound 2 was rapidly distributed for different body organs as a result of rapid clearance from the blood. There is no specific accumulation of radioactivity in the different organs over the time except tumour site. Regarding tumour uptake; [^{131}I] I-compound 2 was gathered in a high ratio reached 13.7 after one hour in comparison with 2.97 at normal muscle at the same time point. Figure 6 shows the target non-target ratios between tumour muscles and normal muscles, and between tumour muscles and blood. This figure declares that one hour time post-injection may be the best time point to use [^{131}I]I- compound 2 as a theranostic agent.

Conclusion

Pyrazole-based analogs play a significant role in the creation of numerous medications and have a wide spectrum of pharmacological actions. Pyrazole derivatives were

synthesized via green methods to be tested for *in-vitro* chemo- and TRT. These substances were synthesized as a result of their noteworthy biological activities, which have made them prospective candidates in the discovery and development of new drugs. The most effective synthesized pyrazole derivative against the two tested cancer cell lines is 4,6-Diamino-1,3-diphenyl-1H-pyrazolo[3,4-b]pyridine-5-carbonitrile which shows high effective action against both HepG2 and HCT-116 cell lines and also it has high accumulation at cancer site which guide us to conclude that this derivative (compound 2) could be used as cancer chemotherapeutic agent. Also, radioiodination of this compound using I-131 -which is used as therapeutic radioisotope- making this compound to be used for TRT. In conclusion the synthesized new pyrazole derivative can be used for chemo/radioisotope therapy after further preclinical studies.

Supplementary Information

The online version contains supplementary material available at https://doi.org/10.1186/s13065-023-01053-7.

Additional file 1. Figure S1. IR spectrum of compound 2. **Figure S2.** ^{1}H-NMR of compound 2. **Figure S3.** MS of compound 2. **Figure S4.** IR spectrum of compound 3. **Figure S5.** ^{1}H-NMR of compound 3. **Figure S6.** ^{13}C-NMR of compound 3. **Figure S7.** MS of compound 3. **Figure S8.** IR spectrum of compound 4. **Figure S9.** ^{1}H-NMR of compound 4. **Figure S10.** MS of compound 4. **Figure S11.** IR spectrum of compound 5. **Figure S12.** ^{1}H-NMR of compound 5. **Figure S13.** MS of compound 5. **Figure S14.** IR spectrum of compound 6. **Figure S15.** ^{1}H-NMR of compound 6. **Figure S16.** ^{13}C-NMR of compound 6. **Figure S17.** MS of compound 6. **Figure S18.** IR spectrum of compound 7. **Figure S19.** ^{1}H-NMR of compound 7. **Figure S20.** ^{13}C-NMR of compound 7. **Figure S21.** MS of compound 7. **Figure S22.** IR spectrum of compound 8. **Figure S23.** ^{1}H-NMR of compound 8. **Figure S24.** ^{13}C-NMR of compound 8. **Figure S25.** MS of compound 8. **Figure S26.** IR spectrum of compound 9. **Figure S27.** ^{1}H-NMR of compound 9. **Figure S28.** ^{13}C-NMR of compound 9. **Figure S29.** MS of compound 9.

Acknowledgements
Not applicable.

Author contributions
KEA, GHS, BME and AAS design the work. KEA and GHS perform the organic synthesis of pyrazole derivatives and in-vitro cytotoxicity assay. AAS and BME perform the radioiodination and pharmacokinetic studies. All authors read and approved the final manuscript.

Funding
Open access funding provided by The Science, Technology & Innovation Funding Authority (STDF) in cooperation with The Egyptian Knowledge Bank (EKB).

Availability of data and materials
All data generated or analyzed during this study are included in this published article and supplementary materials.

Declarations

Ethics approval and consent to participate
All experimental protocols were approved by the Egyptian Atomic Energy Authority animal ethics committee protocol number (219/1210–2022) which follows the principles of European Community guidelines associated with Directive 2010/63/EU on the protection of animals used for scientific purposes. This study was conducted in accordance with the ARRIVE guidelines (https://arriveguidelines.org).

Consent for publication
Not applicable.

Competing interests
The authors declare that they have no competing interests.

Received: 9 July 2023 Accepted: 6 October 2023
Published online: 18 October 2023

References

1. Wan Y, Long J, Gao H, Tang Z. 2-Aminothiazole: A privileged scaffold for the discovery of anti-cancer agents. Eur J Med Chem. 2021;210: 112953.
2. Zhao C, Rakesh K, Mumtaz S, Moku B, Asiri AM, Marwani HM, Manukumar H, Qin H-L. Arylnaphthalene lactone analogues: synthesis and development as excellent biological candidates for future drug discovery. RSC Adv. 2018;8:9487–502.
3. Lucas SW, Qin RZ, Rakesh K, Kumar KS, Qin H-L. Chemical and biology of Sulfur (VI) fluoride exchange (SuFEx) click chemistry for drug discovery. Bioorg Chem. 2022. https://doi.org/10.1016/j.bioorg.2022.106227.
4. Rakesh K, Shantharam C, Sridhara M, Manukumar H, Qin H-L. Benzisoxazole: a privileged scaffold for medicinal chemistry. MedChemComm. 2017;8:2023–39.
5. Rakesh K, Wang S-M, Leng J, Ravindar L, Asiri AM, Marwani HM, Qin H-L. Recent development of sulfonyl or sulfonamide hybrids as potential anticancer agents: A key review. Anticancer Agents Med Chem. 2018;18:488–505.
6. Khan I, Shareef MA, Kumar CG. An overview on the synthetic and medicinal perspectives of indenopyrazoles. Eur J Med Chem. 2019;178:1–12.
7. Sridhara MB, Rakesh KP, Manukumar HM, Shantharam CS, Vivek HK, Kumara HK, Mohammed YH, Gowda DC. Synthesis of dihydrazones as potential anticancer and dna binding candidates: a validation by molecular docking studies. Anticancer Agents Med Chem. 2020;20:845–58.
8. Wang L, Fang K, Cheng J, Li Y, Huang Y, Chen S, Dong G, Wu S, Sheng C. Scaffold hopping of natural product evodiamine: discovery of a novel antitumor scaffold with excellent potency against colon cancer. J Med Chem. 2019;63:696–713.
9. Picconi P, Hind CK, Nahar KS, Jamshidi S, Di Maggio L, Saeed N, Evans B, Solomons J, Wand ME, Sutton JM. New broad-spectrum antibiotics containing a pyrrolobenzodiazepine ring with activity against multidrug-resistant gram-negative bacteria. J Med Chem. 2020;63:6941–58.
10. Yu J, Jia H, Guo X, Desta S, Zhang S, Zhang J, Ding X, Liang X, Liu X, Zhan P. Design, synthesis, and evaluation of novel heteroaryldihydropyrimidine derivatives as non-nucleoside hepatitis B virus inhibitors by exploring the solvent-exposed region. Chem Biol Drug Des. 2020;95:567–83.
11. Ju Z, Su M, Hong J, La Kim E, Moon HR, Chung HY, Kim S, Jung JH. Design of balanced COX inhibitors based on anti-inflammatory and/or COX-2 inhibitory ascidian metabolites. Eur J Med Chem. 2019;180:86–98.
12. Moku B, Ravindar L, Rakesh K, Qin H-L. The significance of N-methylpicolinamides in the development of anticancer therapeutics: Synthesis and structure-activity relationship (SAR) studies. Bioorg Chem. 2019;86:513–37.
13. Rakesh KP, Darshini N, Manukumar HM, Vivek HK, Eissa MY, Prasanna DS, Mallesha N. Xanthone conjugated amino acids as potential anticancer and DNA binding agents: molecular docking, cytotoxicity and sar studies. Anticancer Agents Med Chem. 2018;18:2169–77.
14. Cherrak K, Khamaysa O, Bidi H, El Massaoudi M, Ali IA, Radi S, El Ouadi Y, El-Hajjaji F, Zarrouk A, Dafali A. Performance evaluation of newly synthetized bi-pyrazole derivatives as corrosion inhibitors for mild steel in acid environment. J Mol Struct. 2022;1261:132925.
15. Kanwal I, Rasool N, Zaidi SHM, Zakaria ZA, Bilal M, Hashmi MA, Mubarik A, Ahmad G, Shah SAA. Synthesis of functionalized thiophene based pyrazole amides via various catalytic approaches: Structural features through

computational applications and nonlinear optical properties. Molecules. 2022;27:360.
16. Kurt A, Koca M. Synthesis, characterization and thermal degradation kinetics of a new pyrazole derived methacrylate polymer, poly (1, 3-diphenyl-1H-pyrazol-5-yl methacrylate). Acta Chim Slov. 2022;69:466–77.
17. El Arrouji S, Karrouchi K, Warad I, Berisha A, Alaoui KI, Rais Z, Radi S, Taleb M, Ansar M, Zarrouk A. Multidimensional analysis for corrosion inhibition by new pyrazoles on mild steel in acidic environment: Experimental and computational approach. Chemical Data Collections. 2022;40:100885.
18. Cherrak K, El Massaoudi M, Outada H, Taleb M, Lgaz H, Zarrouk A, Radi S, Dafali A. Electrochemical and theoretical performance of new synthetized pyrazole derivatives as promising corrosion inhibitors for mild steel in acid environment: molecular structure effect on efficiency. J Mol Liq. 2021;342:117507.
19. Bekhit AA, Nasralla SN, El-Agroudy EJ, Hamouda N, Abd El-Fattah A, Bekhit SA, Amagase K, Ibrahim TM. Investigation of the anti-inflammatory and analgesic activities of promising pyrazole derivative. Eur J Pharm Sci. 2022;168:106080.
20. Le TG, Kundu A, Ghoshal A, Nguyen NH, Preston S, Jiao Y, Ruan B, Xue L, Huang F, Keiser J. Novel 1-methyl-1 h-pyrazole-5-carboxamide derivatives with potent anthelmintic activity. J Med Chem. 2019;62:3367–80.
21. Mor S, Khatri M, Sindhu S. Recent progress in anticancer agents incorporating pyrazole scaffold. Mini Rev Med Chem. 2022;22:115–63.
22. Sangwan S, Singh R, Gulati S, Rana S. Efficient and facile synthesis of pyrazoles using Guar-gum as organocatalyst and their in vitro herbicidal activity. Curr Res Green Sustain Chem. 2021;4:100146.
23. Karati D, Mahadik KR, Kumar D. Pyrazole Scaffolds: centrality in anti-inflammatory and antiviral drug design. Med Chem. 2022. https://doi.org/10.2174/1573406418666220410181827.
24. Chalkha M, Akhazzane M, Moussaid FZ, Daoui O, Nakkabi A, Bakhouch M, Chtita S, Elkhattabi S, Housseini AI, El Yazidi M. Design, synthesis, characterization, in vitro screening, molecular docking, 3D-QSAR, and ADME-Tox investigations of novel pyrazole derivatives as antimicrobial agents. New J Chem. 2022;46:2747–60.
25. Ravindar L, Hasbullah SA, Rakesh K, Hassan NI. Pyrazole and pyrazoline derivatives as antimalarial agents: A key review. Eur J Pharm Sci. 2022;183:106365.
26. Verma R, Verma SK, Rakesh KP, Girish YR, Ashrafizadeh M, Kumar KSS, Rangappa KS. Pyrazole-based analogs as potential antibacterial agents against methicillin-resistance *Staphylococcus aureus* (MRSA) and its SAR elucidation. Eur J Med Chem. 2021;212:113134.
27. Dong P, Rakesh K, Manukumar H, Mohammed YHE, Karthik C, Sumathi S, Mallu P, Qin H-L. Innovative nano-carriers in anticancer drug delivery-a comprehensive review. Bioorg Chem. 2019;85:325–36.
28. Varluvothu A, Vaarla K, Vermeire K, Leelavathi P. Microwave-assisted one-pot multicomponent synthesis of 2-(-4-oxo-2-(1-(2-oxo-2h-chromen-3-yl) ethylidene) hydrazono) thiazolidin-5-yl) acetic acid derivatives and their antiviral activity. J Heterocycl Chem. 2022;59(9):1604–15.
29. Prasanna BL, Rao BS, Lavanya P, Maddila S. A green, an efficient and viable approach for the synthesis of novel 4H-pyran-indolin-2-one derivatives via a one-pot reaction by grinding method. Chem Data Collect. 2022;37:100804.
30. Yun ES, Akhtar MS, Mohandoss S, Lee YR. Microwave-assisted annulation for the construction of pyrido-fused heterocycles and their application as photoluminescent chemosensors. Org Biomol Chem. 2022;20:3397–407.
31. Anwer KE, El-Sattar NEA, Shamaa MM, Zakaria MY, Beshay BY. Design, green synthesis and tailoring of vitamin E TPGS augmented niosomal nano-carrier of pyrazolopyrimidines as potential anti-liver and breast cancer agents with accentuated oral bioavailability. Pharmaceuticals. 2022;15:330.
32. Schmidt J, Wölker J, Lippmann P, Ott I. Microwave assisted synthesis of rhodium (I) N-heterocyclic carbene complexes and their cytotoxicity against tumor cell lines. J Organomet Chem. 2022;964:122300.
33. Anwer KE, Sayed GH, Ramadan RM. Synthesis, spectroscopic, DFT calculations, biological activities and molecular docking studies of new isoxazolone, pyrazolone, triazine, triazole and amide derivatives. J Mol Struct. 2022;1256:132513.
34. Essa BM, Selim AA, Sayed GH, Anwer KE. Conventional and microwave-assisted synthesis, anticancer evaluation, 99mTc-coupling and In-vivo study of some novel pyrazolone derivatives. Bioorg Chem. 2022;125:105846.
35. Anwer KE, Farag AA, Mohamed EA, Azmy EM, Sayed GH. Corrosion inhibition performance and computational studies of pyridine and pyran derivatives for API X-65 steel in 6 M H2SO4. J Ind Eng Chem. 2021;97:523–38.
36. Farag AA, Mohamed EA, Sayed GH, Anwer KE. Experimental/computational assessments of API steel in 6 M H2SO4 medium containing novel pyridine derivatives as corrosion inhibitors. J Mol Liq. 2021;330:115705.
37. Mohamed SS, Shabaan SN, Abdelghaffar NF, Dauoud NT, Sayed GH, Anwer KE. Synthesis and exploring novel annulated 1, 3-diphenylpyrazole derivatives as antimicrobial and anticancer agents. J Basic Environ Sci. 2021;8:124–39.
38. Anwer KE, Sayed GH. Conventional and microwave reactions of 1, 3-diaryl-5, 4-enaminonitrile-pyrazole derivative with expected antimicrobial and anticancer activities. J Heterocycl Chem. 2020;57:2339–53.
39. Sayed GH, Azab ME, Anwer KE. Conventional and microwave-assisted synthesis and biological activity study of novel heterocycles containing pyran moiety. J Heterocycl Chem. 2019;56:2121–33.
40. Sayed GH, Azab ME, Anwer KE, Raouf MA, Negm NA. Pyrazole, pyrazolone and enaminonitrile pyrazole derivatives: Synthesis, characterization and potential in corrosion inhibition and antimicrobial applications. J Mol Liq. 2018;252:329–38.
41. Jimenez C, Erwin W, Chasen B. Targeted radionuclide therapy for patients with metastatic pheochromocytoma and paraganglioma: from low-specific-activity to high-specific-activity iodine-131 metaiodobenzylguanidine. Cancers. 2019;11:1018.
42. Jha A, Taïeb D, Carrasquillo JA, Pryma DA, Patel M, Millo C, de Herder WW, Del Rivero J, Crona J, Shulkin BL. High-specific-activity-131I-MIBG versus 177Lu-DOTATATE targeted radionuclide therapy for metastatic pheochromocytoma and paragangliomahigh-specific-activity 131I-MIBG vs. 177Lu-DOTATATE. Clin Cancer Res. 2021;27:2989–95.
43. Mohamed S, Dawoud N, Shabaan SN, Fathall N, Hosni G, Anwer KE. Synthesis and biological activity of a new class of enaminonitrile pyrazole. Egypt J Chem. 2021;64:3187–203.
44. Mishra D, Singh R, Rout C. Synthesis of highly functionalized pyrazoles using AlCl 3 as catalyst. J Chem Pharm Res. 2017;9:16–9.
45. Aljuhr SA, Abdelaziz G, Selim AA, Zaghary WA, Sakr TM. Anti-cancer, anti-inflammatory and antioxidant effects of Vit-A/C@ SeNPs in mutual diethylnitrosamine and carbon tetrachloride induced hepatocellular damage in albino rats. J Drug Deliv Sci Technol. 2022;75:103723.
46. Selim AA, Motaleb M, Fayez HA. Lung cancer-targeted [131I]-Iodoshikonin as theranostic agent: radiolabeling, in vivo pharmacokinetics and biodistribution. Pharm Chem J. 2022;55:1163–8.
47. Essa BM, Selim AA, El-Kawy O, Abdelaziz G. Preparation and preliminary evaluation study of [131I] iodocolchicine-gallic-AuNPs: a potential scintigraphic agent for inflammation detection. Int J Radiat Biol. 2022. https://doi.org/10.1080/09553002.2022.2047824.
48. Essa BM, Abd-Allah WH, Sakr TM. Synthesis, 99mTc-labeling, in-vivo study and in-silico investigation of 6-amino-5-[(bis-(2-hydroxy-ethyl)-amino] methyl] 2-methyl pyrimidin-4-ol as a potential probe for tumor targeting. J Radioanal Nucl Chem. 2022. https://doi.org/10.1007/s10967-022-08412-z.
49. Wang F, Zeng J, Tian X, Gao H, Sukmanov V. Effect of ultrafine grinding technology combined with high-pressure, microwave and high-temperature cooking technology on the physicochemical properties of bean dregs. LWT. 2022;154:112810.
50. Adewuyi SO, Ahmed HA. Grinding behaviour of microwave-irradiated mining waste. Energies. 2021;14:3991.
51. Huang W, Liu Y. Study on microwave-assisted grinding and liberation characteristics for ludwigite. J Microw Power Electromagn Energy. 2021;55:28–44.
52. Fayez H, El-Motaleb MA, Selim AA. Synergistic cytotoxicity of shikonin-silver nanoparticles as an opportunity for lung cancer. J Labelled Compd Radiopharm. 2020;63:25–32.
53. Abdelaziz G, Shamsel-Din HA, Sarhan MO, Gizawy MA. Tau protein targeting via radioiodinated azure A for brain theranostics: radiolabeling, molecular docking, in vitro and in vivo biological evaluation. J Labelled Compd Radiopharm. 2020;63:33–42.
54. Saha GB. Physics and radiobiology of nuclear medicine. New York: Springer Science & Business Media; 2012.

Publisher's Note